



UNITED NATIONS
UNIVERSITY

UNU-GTP

Geothermal Training Programme

Orkustofnun, Grensasvegur 9,
IS-108 Reykjavik, Iceland

Reports 2017
Number 17

NUMERICAL MODELLING OF GEOTHERMAL RESERVOIR IN DONGLI LAKE AREA, CHINA

Liu Donglin

Tianjin Geothermal Exploration and Development Designing Institute
189 Weiguo Road, Hedong District 300250
Tianjin
P.R. CHINA
529393809@qq.com

ABSTRACT

Dongli Lake geothermal system is a typical low- to medium-temperature sedimentary basin where a traversing fault conducts heat and fluid. Most of the geothermal wells are distributed along this fault. Various data were collected for this study, such as seismic profiles, drilling data, stratigraphic data and historical dynamic monitoring data. A 3D geological model was established using Leapfrog Geothermal software, the best place for drilling was located and two wells were sited on the western part of the study area. Since there is no obvious hydraulic connection between the western and eastern sides of the fault, the western part was chosen for more specific study due to the well known geology and production history. Based on the conceptual model, a numerical model of the study area was created with PetraSim. Numerical model was calibrated to reach the natural state, therefore the model parameters can be used as initial conditions for production. After the numerical model calibration, the observed and simulated data showed a good match. The mean relative error of the temperature simulation is 33% while the mean relative error for pressure simulation is 9.7%. The calibration result of Jxw reservoir's X, Y permeability is $3.0 \times 10^{-13} \text{ m}^2$, the Z permeability is $3.0 \times 10^{-14} \text{ m}^2$ and wet heat conductivity is $2.9 \text{ W}/(\text{m} \cdot \text{K})$.

1. INTRODUCTION

The main purpose of modelling geothermal resources is to forecast the response of a geothermal system to different production scenarios, to estimate the capacity of the system and to evaluate the influence of different development actions, which will provide a basis for future management (Axelsson, 2010). It is a direct way to gather information, achieve better understanding of the geothermal system properties and natural state, and help to determine a reasonable exploitation of the resource (Axelsson, 2013). Modelling is one of the main methods of geothermal reservoir physics, which is used to analyse different types of data, such as transient pressure and temperature logging data, with the purpose of estimating reservoir properties, such as permeability and thermal conductivity (Axelsson, 2013).

Once reservoir properties have been estimated, models are used to simulate the conditions and changes in the geothermal system, both during the pre-exploitation stage without a source and sink (natural state) and development condition (production state). Modelling is the most efficient ways to understand the

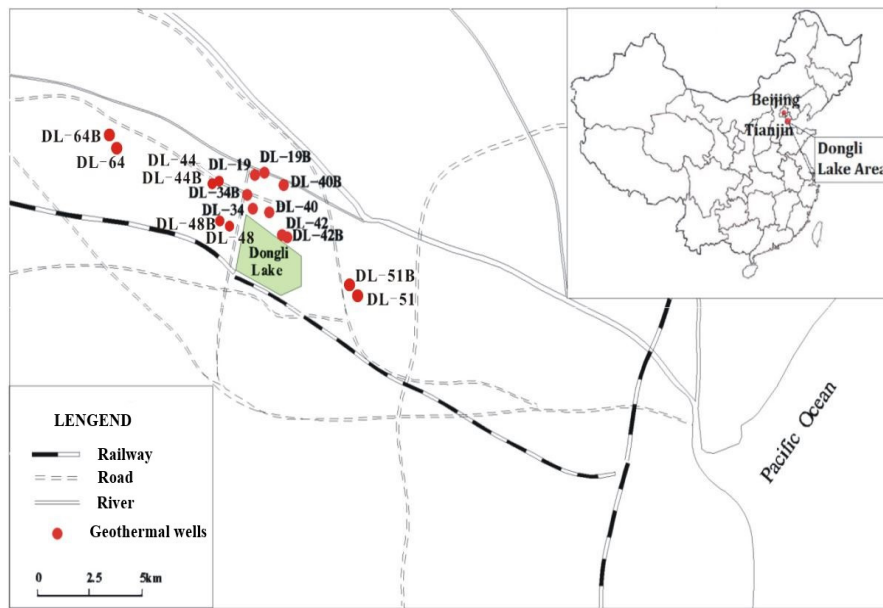


FIGURE 1: Map of the study area (Wang, 2016)

nature of geothermal systems, as well as being the most powerful method to determine reservoir response to future development (Axelsson, 2008).

The Dongli Lake area is located in Tianjin Binhai new district and covers an area of 69 km² (Figure 1).

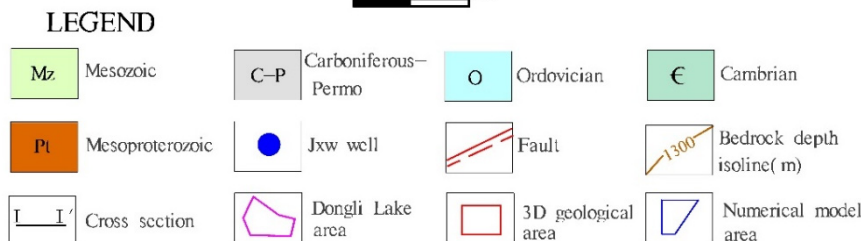
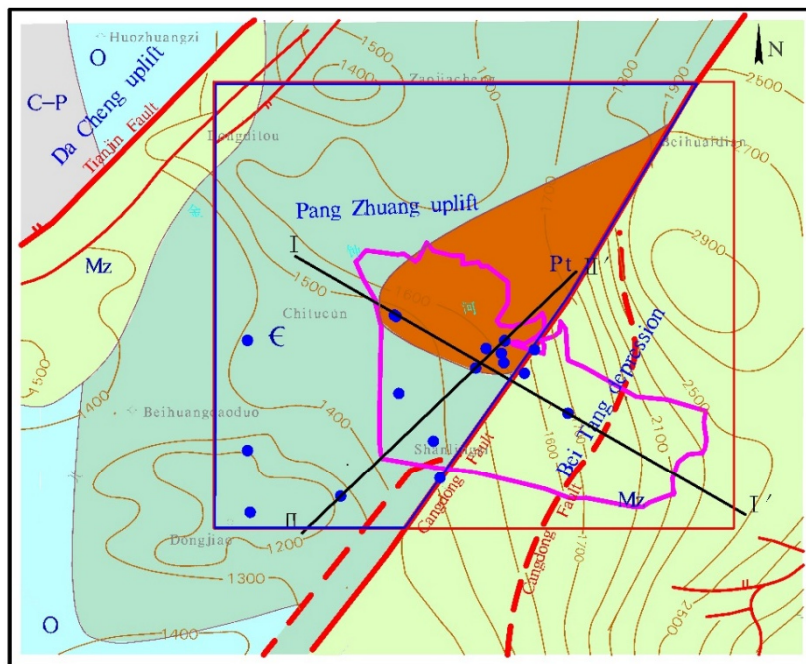


FIGURE 2: Geological formations and structures of the study area

This area has abundant low- to medium-temperature geothermal resources, which are stored in porous sedimentary reservoirs and bedrock (Duan et al., 2011). The highest-temperature fluid is stored in the Jxw reservoir. The Jxw reservoir is hosted mainly in Mesoproterozoic dolomitic limestone, which belongs to semi-open and semi-closed bedrock subsystems, where geothermal karst fluids exist. Most of the geothermal wells were drilled to the depth of this reservoir near the Cangdong fault (Figure 2) (Tian, 2014). The geothermal water is mostly used for space heating during winter and a small proportion of it is used for bathing and agriculture (Zong et al., 2016).

To study the flow paths and predict cooling due to long-term injection, a tracer test was performed on the 17th of December 2015, when 700 kg of ammonium molybdate (Mo) was injected into well DL-48B (Figure 1). No obvious tracer recovery was detected in the water samples collected during the 90 days of the tracer test within the Dongli Lake area (Wang, 2016).

The volumetric method previously has been applied in Dongli Lake area and the calculation results showed that the recoverable heat of Jxw reservoir is 2.82×10^9 GJ, which means that there is a great potential for geothermal heat in this area (Tian, 2014). The volumetric method is often used for the first stage of assessment, when data are limited. However, this method does not take into consideration the dynamic response of a reservoir, such as the pressure response, permeability, recharge, etc. (Axelsson, 2008).

For a better understanding of the geothermal conditions of this area, a smaller zone within Dongli Lake region was chosen for this study (Figure 2). Based on the data analysis, a 3D geological model of the study area was created using Leapfrog geothermal software (Leapfrog, 2017). The area with the most intensive production and injection is located on the western part of the Cangdong fault (Figure 2) and was chosen for the numerical simulation using PetraSim (Thunder Head Engineering, 2015). The aim of this project is to make the calibrated numerical model, so its parameters can be used as initial conditions for the production state.

2. BACKGROUND

2.1 Geological setting of the study area

The study area is located northeast of the Shan Lingzi geothermal field, the tectonic location is on the Pang Zhuang uplift and Bei Tang depression. The Cangdong fault divides the study area into two parts (Figure 2). The western part is in the Pan Zhuang uplift; the bedrock surface is Mesozoic, Palaeozoic Cambrian and Mesoproterozoic-based, and the depth of bedrock surface is at 1430 ~ 1750 m (Figure 3). The eastern part is in the Bei Tang depression; the bedrock surface is Mesozoic, and the depth of the bedrock surface is 1500 ~ 2500 m, increasing from the fault zone to the east within the study area (Figure 4).

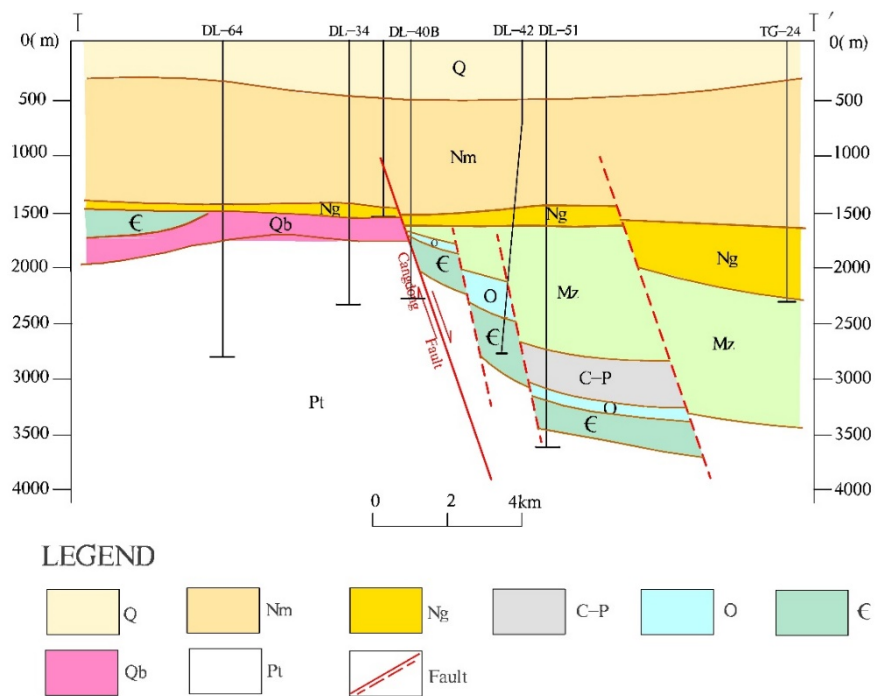


FIGURE 3: Geological cross-section I-I', location see Figure 2

The Pan Zhuang uplift is a long fault block for the north-easterly spread in the plane, Tianjin fault and Cangdong fault are the boundaries to the northwest and southeast, respectively, and it is adjacent to the Da Cheng uplift and Bei Tang depression. Mesozoic, Palaeozoic Ordovician, Cambrian and

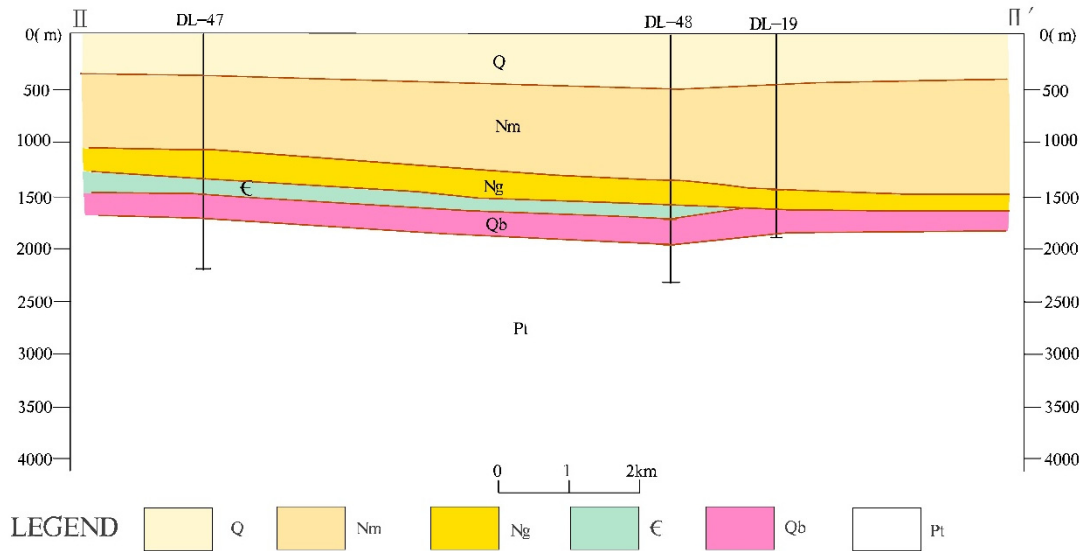


FIGURE 4: Geological cross-section II-II', location see Figure 2

Mesoproterozoic rocks dominate the bedrock surface on the Pan Zhuang uplift, and the depth of bedrock increases from the Northeast to South-West (Tianjin Bureau of Geology, 1992).

2.2 Temperature gradient in the area

The cap rock temperature has a direct relationship with the magmatic activity, geological structure and hydrogeological background, therefore a temperature gradient anomaly usually occurs near a structural fault belt, especially in a raised area.

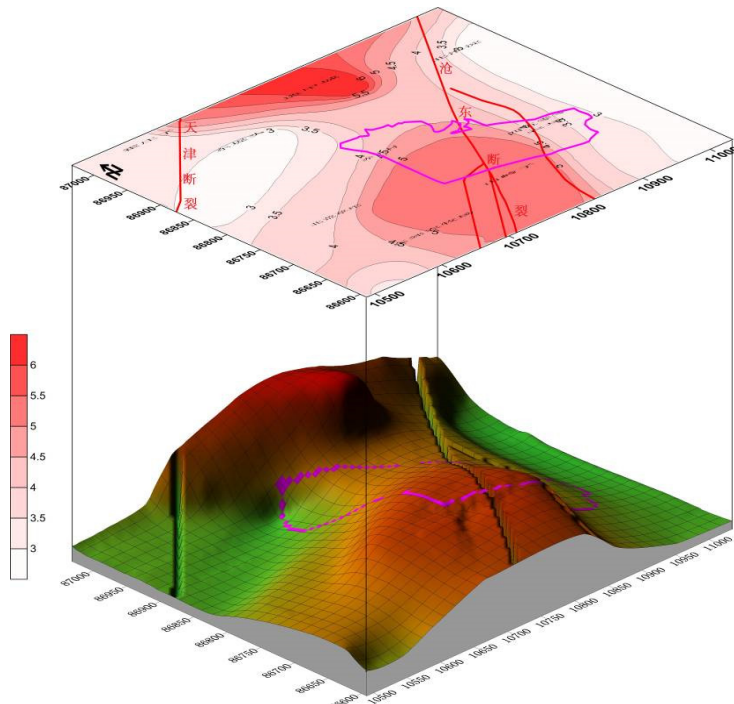


FIGURE 5: Distribution of temperature gradient in the study area

Based on the average temperature gradient of each geothermal well in the study area, a geothermal gradient map of the cap rock was prepared using Surfer 13 (Figure 5). The map shows that the study area is located in the area of high heat flow at the Pang Zhuang uplift (Figure 2). The average geothermal gradient of the cap rock is 3.0-5.4°C/100 m. The highest geothermal gradient in the cap rock is located near the Cangdong fault, which can conduct water and heat from deeper layers. The geothermal gradient gradually decreases with increasing distance from Cangdong fault, i.e. from more than 5.0°C/100 m near Cangdong fault to less than 3.0°C/100 m about 5 km away from the fault.

The geothermal gradient value decreases with increasing depth (Figure 6). The main reason for that is that the thermal conductivity is

controlled by the formation lithology and the geothermal gradient has a negative relationship with the rock thermal conductivity.

It is observed that the Quaternary bedrock in the study area is high in argillaceous components, has loose structure and low porosity hence, the thermal conductivity is low as well. The Neogene sandstone has higher density than the Quaternary bedrock, so the thermal conductivity increases accordingly. In addition, the groundwater flow improves thermal conductivity of the rock and the gradient value is lower, which indicates that the change of formation lithology and groundwater activity transformed the vertical geothermal field. At the same time, the fault and other main structures can conduct water and affect the vertical change of ground temperature. These changes reflect the characteristics of the geothermal field, being either controlled by convection or conduction.

According to the temperature logging data shown in Figure 6, the temperature of the geothermal wells gradually increase with increasing depth. But the temperature increase of the bedrock is relatively slow because of the vertical convection and high thermal conductivity.

2.3 Production in the study area

The geothermal production in Dongli Lake geothermal field started over 30 years ago. The first geothermal well DL-19 (Jxw) (Figure 1) was drilled in 1986 (Zhao, 2010). It was an artesian well at first, but due to economic development, hot water demand for space heating and increasing tourism, the pressure of the geothermal reservoir dropped annually.

By the end of 2016, there were 24 geothermal wells in this area, including 17 wells in the Jxw geothermal reservoir; nine production wells and eight injection wells (Table 1). In 2008 and 2009, the total annual production and injection were $59.4 \times 10^4 \text{ m}^3$ and $53.4 \times 10^4 \text{ m}^3$, respectively (Zhao, 2010). In 2012, the total production rapidly increased and reached $140.7 \times 10^4 \text{ m}^3$ (Zong et al., 2016). In 2013, the production increased to $157.4 \times 10^4 \text{ m}^3$, with a slight decrease in the production in 2014, to $147 \times 10^4 \text{ m}^3$. In 2015, the production increased to $162.3 \times 10^4 \text{ m}^3$, while in 2016, the production jumped to $182.4 \times 10^4 \text{ m}^3$.

Because of the intensive development of the geothermal resources, the water level gradually declined in well DL-19 after 2007 (Figure 7). The wells are used only during wintertime, i.e. from November 15th until March 15th, so the water level fluctuates significantly between seasons. According to the dynamic monitoring data from 2007, the static water level in the Jxw reservoir was about 100 m depth, while in 2016 it was at around 140 m depth. Hence, the annual decline is about 4 m/year (Zong et al., 2016).

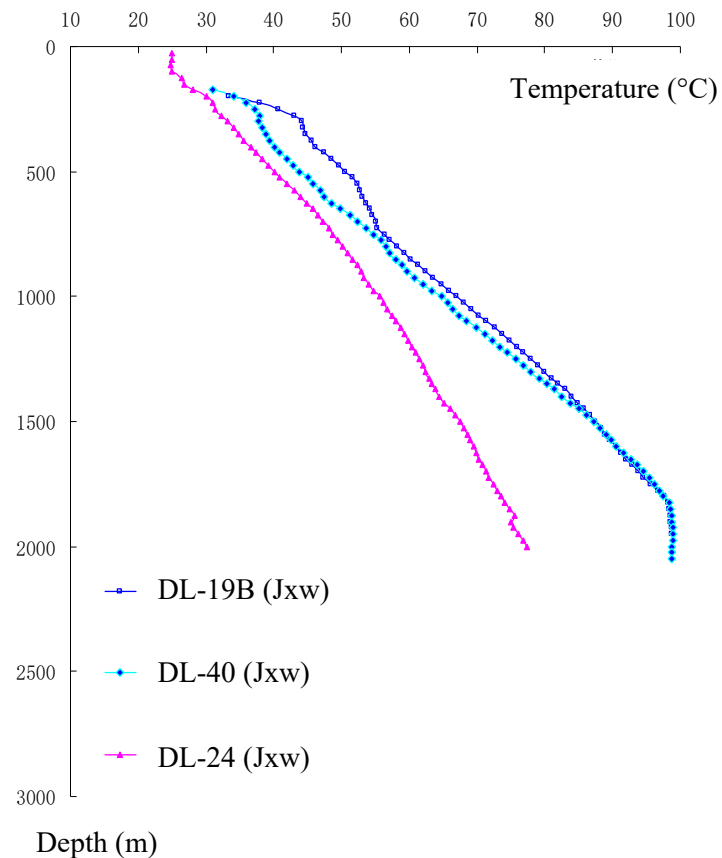


FIGURE 6: Temperature logging of three wells in the study area

TABLE 1: Details of geothermal wells in the Dongli Lake area (Jxw reservoir) (Zong et al., 2016)

Well	Reservoir	Depth (m)	Out-flow temp. (°C)	Flow rate (m ³ /h)	Thickness (m)	
DL-44	Jxw	2373	98	112.8	462	
DL-44B		2495	98	112.8	468	
DL-34		2327	100	204.6		
DL-34B				96.5	140	
DL-19		1842	83	49.2		
DL-19B		2384	88	118		
DL-40		2328	98.5	126	534	
DL-40B		2279	101	126	509	
DL-51		3634	97	70.7	153	
DL-48		2329	93	122	374	
DL-48B		2534	93	112.8	671	
DL-64		2565	93	126	798.6	
DL-64B		2784	96	119	1031.8	
DL-69		2510	94	126	560	
DL-69B		2666	92	140.2	624	
DL-76		2397	91	133	719	
DL-76B		2509	91	140.2	546.5	

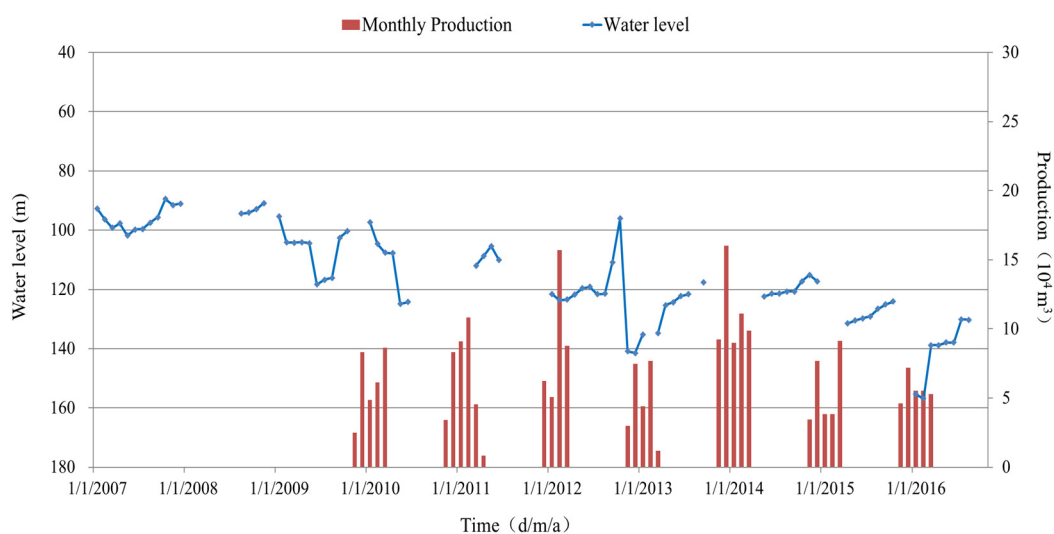


FIGURE 7: Water level and monthly production of DL-19 from 2007 to 2016

3. 3D GEOLOGICAL MODEL

A geological model is the basis of a comprehensive geothermal model. A 3D geological model with different integrated data is a direct and effective way to study the geothermal reservoir (Gunnarsdóttir and Poux, 2015). For the 3D geological model, a 300 km² area was selected (Figure 1). It should be noted that the bottom depth of the Jxw layer is defined as 4000 m. The targets for the 3D geological model were rather simple:

1. To compile all relevant data on geothermal research and boreholes;
2. To build a simple stratigraphic and structural model.

3.1 Data collection

Due to economic development, many geothermal wells had been drilled in this area in the last decade. The data gathered from different sources are listed in Table 2.

All the data were converted to the WGS-84 geographic coordinate system in metres before they were imported into the model. The elevation data were gained from Google Earth, the elevation ranges from -2 to 8 m above sea level.

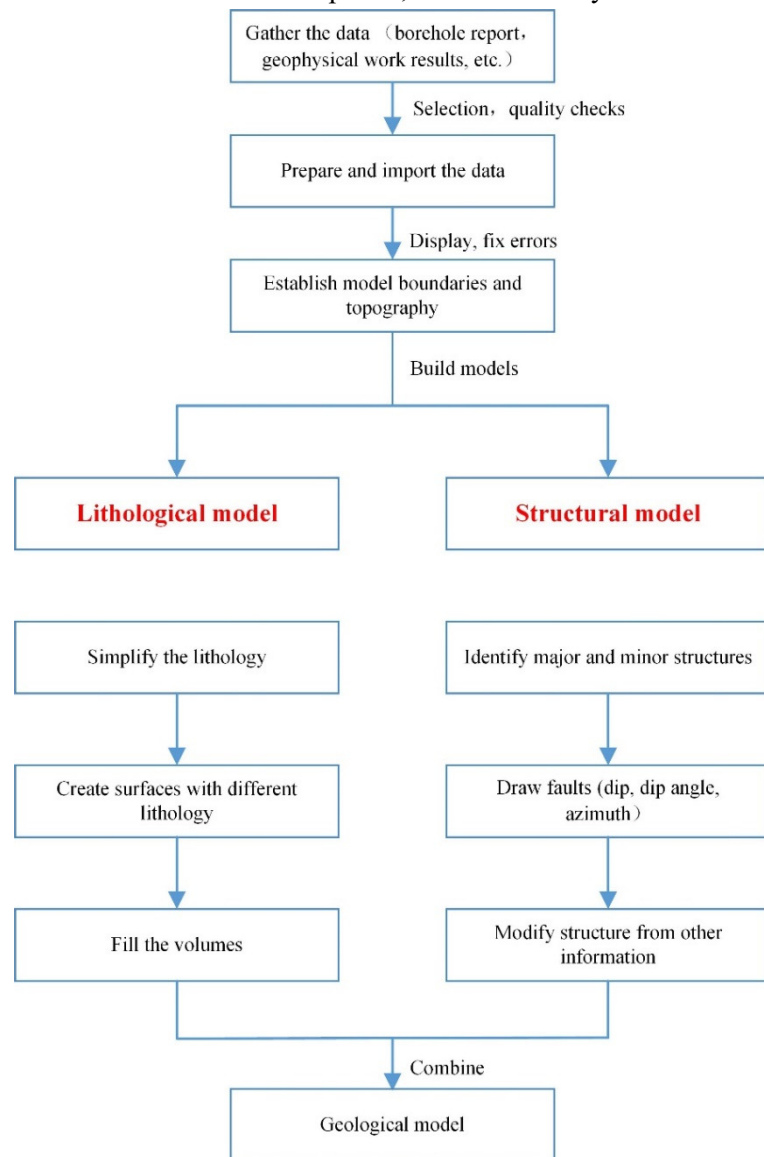
TABLE 2: Data collection in the study area

Type	Quantity
Seismic profiles	2
Drilling stratigraphic data	24
Drilling logs	5
Rock core analysis	5
Borehole completion report	4

3.2 Work flow of the 3D geological model

The first phase of the project consisted of gathering the available data, which came in different formats and from different sources. Therefore, the primary task was to evaluate what was available and to select the most useful and the best quality ones. Once that task was completed, it was necessary to create files that could be imported into the Leapfrog software in the correct format and then to check for any errors or missing data (Gunnarsdóttir and Poux, 2015).

Before starting work on the models, all the available data were integrated and checked in Leapfrog, the model boundaries (including the topography) were defined according to the geological structure, the available data and the specific interests for some areas. The workflow diagram is presented in Figure 8 (Gunnarsdóttir and Poux, 2015).



3.3 Stratigraphic model

The main purpose of Leapfrog is to build 3D model from geological data or other data from wells and surveys. Two models of the study area were built using the available data. The stratigraphy model developed for the study area is presented in Figure 9. The different strata are as follows:

- 1) Quaternary (Q): This stratum is widely distributed in the study area. The lithology is alluvial-dilluvial faces clay and sand layer. The exposure thickness is 280 ~ 320 m.

FIGURE 8: Working flow chart for a geological model (Gunnarsdóttir and Poux, 2015)

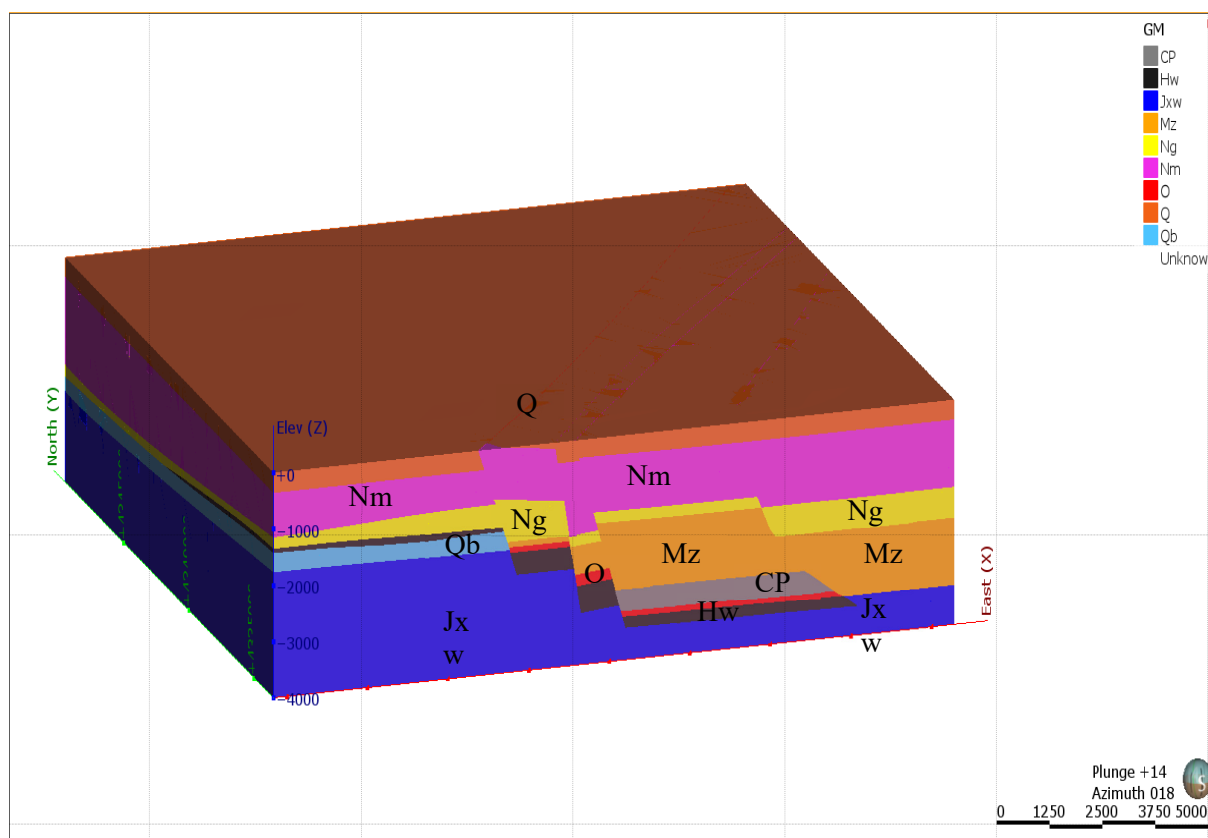


FIGURE 9: A 3D stratigraphy model of the study area

- 2) Minghuazhen formation (Nm): This stratum is widely distributed in the study area. The upper lithology is semi-cemented fine sand and fine sandstone with variegated mudstone. The lower lithology is mainly mudstone with fine siltstone. Drilling reveals that the buried depth of the bottom layer is 1394 ~ 1598 m.
- 3) Guantao formation (Ng): This stratum is widespread in the study area. The lithology is mainly fine siltstone and glutenite. Drilling reveals that the buried depth of the bottom plate is at 1430 ~ 1676 m.
- 4) Mesozoic (Mz): This stratum is unevenly distributed in the study area, it is only distributed to the east of the Cangdong fault. Drilling reveals that the buried depth of the bottom plate is from 1650 to 2630 m. The depth increases gradually to the east.
- 5) Carboniferous-Permian (C-P): This stratum is distributed to the east of the Cangdong fault in the study area, but it is missing near the fault. At present, only well DL-51 penetrates into this layer in the Dongli Lake area, revealing that the buried depth of the bottom plate is about 3100 m, and the exposure thickness about 412 m.
- 6) Ordovician (O): This stratum is mainly distributed to the east of the Cangdong fault in the study area and it is not present to the west of the fault. Drilling reveals that the buried depth of the bottom plate is from 1696 to 3191 m, and the exposure thickness is from 22 to 419 m.
- 7) Cambrian (Hw): This stratum is unevenly distributed in the study area, and is partly absent on the west side of the Cangdong fault. To the west of the fault, the buried depth of the bottom plate is 1720 ~ 1920 m, and the exposure thickness is 74 ~ 324 m. The buried depth of the bottom plate is 2760 ~ 3481 m, and the exposure thickness is 238 ~ 290 m.
- 8) Qingbaikou formation (Qb): This stratum is widely distributed to the west of the Cangdong fault, while to the east it is deeply buried and has not been exposed yet. The buried depth of the bottom plate is 1752 ~ 2016 m, and the exposure thickness is 66 ~ 336 m.
- 9) Jixian Wumishan formation (Jxw): This stratum is widespread in the study area. The buried depth of the roof is at 1752 ~ 2016 m to the west of the Cangdong fault, and the exposure thickness is 480 ~ 1032 m. At present, only well DL-51 penetrates into the layer to the east of the Cangdong

fault. There, the buried depth of the roof is 3481 m, and the exposure thickness is 153 m. The depth to the east towards Beitang depression is generally greater than 4000 m, and, at present, no geothermal wells have been drilled there.

3.4 Structural model of the Cangdong fault zone

Different kind of data, including seismic profiles, drilling records and cutting analysis, were considered for delineating the Cangdong fault (Figure 10). The Cangdong fault is a normal fault and the western plate is the uplifting part, the fault formed in the Yan Shan period and is usually followed by secondary fractures. The fault trend is north-northeast, the dip to south-SSE, the dip angle is between 30 and 48°, and the strata drop 1000 ~ 6000 m.

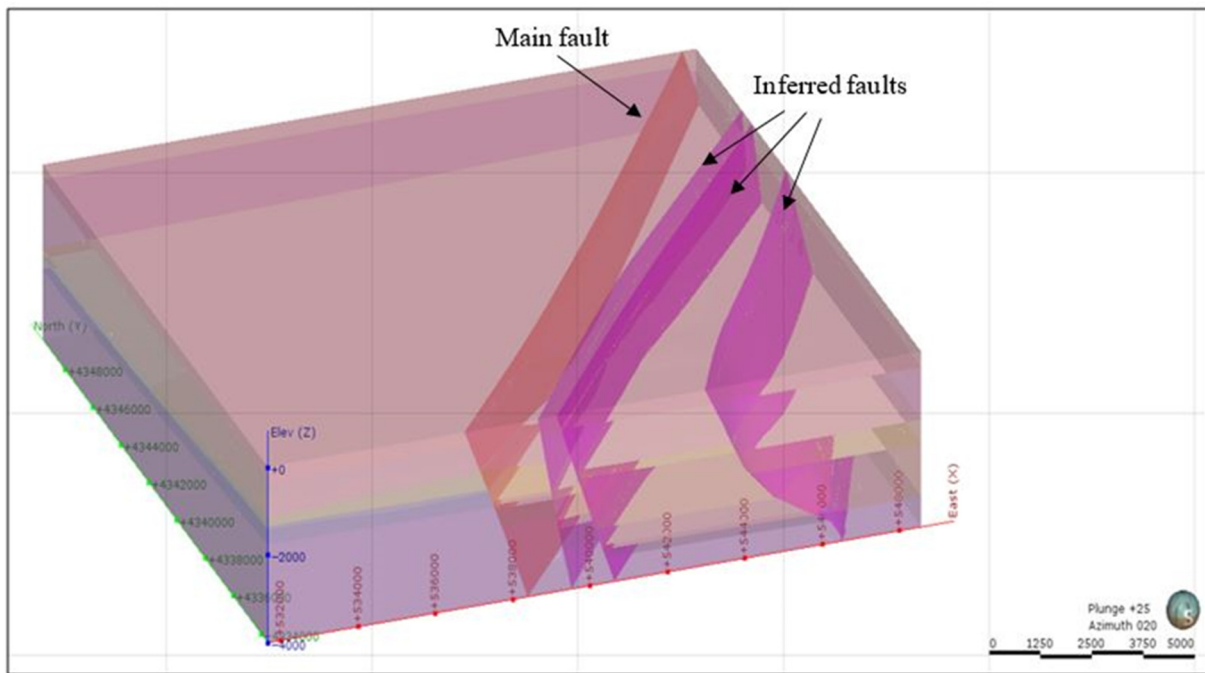


FIGURE 10: A 3D structural model of the study area

Cangdong fault is the boundary of the Cang Xian uplift and the Huang Hua depression. The fault transfers heat and water from the deeper part of the geothermal reservoir to the shallower part, and the influence range is weakened away from the fault zone. The DL-40B and DL-40 geothermal wells (Figure 1) in the Dongli Lake area expose the fracture, and the water temperatures of the two wells reach 102 and 98.5°C, respectively. According to oilfield drilling data, the broken horizontal distance of the fault in Jxw reservoir is more than 800 m.

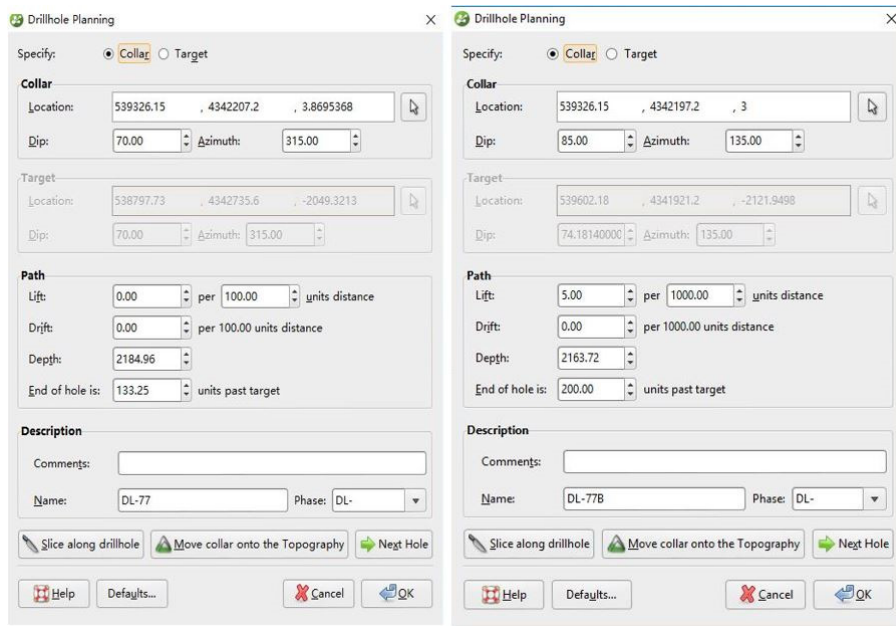
The west side of the study area is located in the upthrow of the fault, and due to the erosion, the bedrock from Mesozoic to Palaeozoic Cambrian is missing. The east side of the fault is the down-throw plate, there the stratigraphy is complete (Mesozoic) and its depth gradually increases to the east.

TABLE 3: Drilling layer depth prediction for planned wells

3.5 Well planning

Prior to drilling, the *Leapfrog geothermal* model was used to predict the geology likely to be encountered by new wells which had been sited (DL-77, DL-77B) (Figures 11 and 12), taking into account a range of drilling scenarios, including (bottom hole) depth (Table 3), dip angle, well azimuth etc. Subsequently, new data can

GM	DL-77	DL-77B
Q	400	402
Nm	1401	1420
Ng	1537	1556
Hw	1640	1636
Qb	2081	2069
Jxw	2385	2364



be added to this model as drilling proceeds, which is of immediate value to the manager, and supports a flexible drilling strategy.

FIGURE 11: Indicative well planning spreadsheet

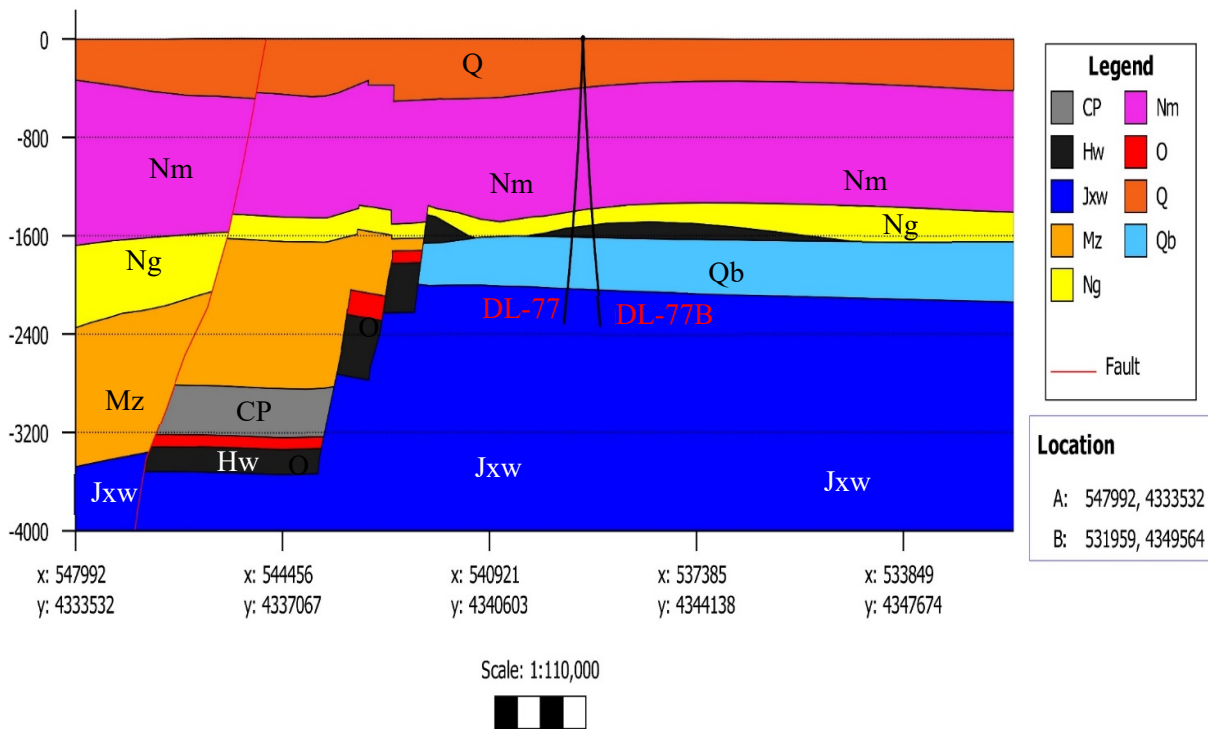


FIGURE 12: Geological cross-section including planned wells

4. NUMERICAL MODELLING

4.1 Conceptual model

Conceptual models are descriptive models incorporating and unifying the essential physical features of the systems in question (Grant et al., 1982). The integration of different disciplines involved in geothermal analysis and development is of great importance (Axelsson, 2013). Conceptual models are an important basis for field development plans, i.e. in siting wells to be drilled and they are the

foundation for all geothermal resource assessments and predictions, particularly volumetric assessments and numerical modelling (Axelsson, 2012).

4.1.1 Jxw conceptual model in Tianjin

The conceptual model of the Jxw geothermal system was constructed on the basis of the research. In the model, the structure of the geothermal system, the heat source, cap rock, hot water flow paths and recharge paths are described. The model is shown in Figure 13.

The main parts of the conceptual model are described as follows:

1. Heat source

The heat source is a result of geothermal conduction due to the radioactive decay of radioactive elements in the deep granite crust and the upper mantle lava flows. One part of the heat of this decay comes from the upper mantle lava flow, while the other part comes from granite at depths of 8~16 km.

2. Water source

According to the regional isotope and hydrogeochemical analysis data, atmospheric precipitation in the Tianjin northern mountains is the main source of geothermal fluids. After the atmospheric precipitation and surface water infiltration the water travels along a channel of faults, joint fissures and the formation pores where it is heated up and turns into geothermal fluid.

3. Thermal reservoir

There are two types of geothermal reservoirs in the Tianjin area, i.e. porous Neogene formations and bedrock with karst fissures. The highest outflow temperature is from the Jxw reservoir. The Jxw reservoir is semi-open and semi-closed bedrock subsystems type, where the geothermal karst fluids exist.

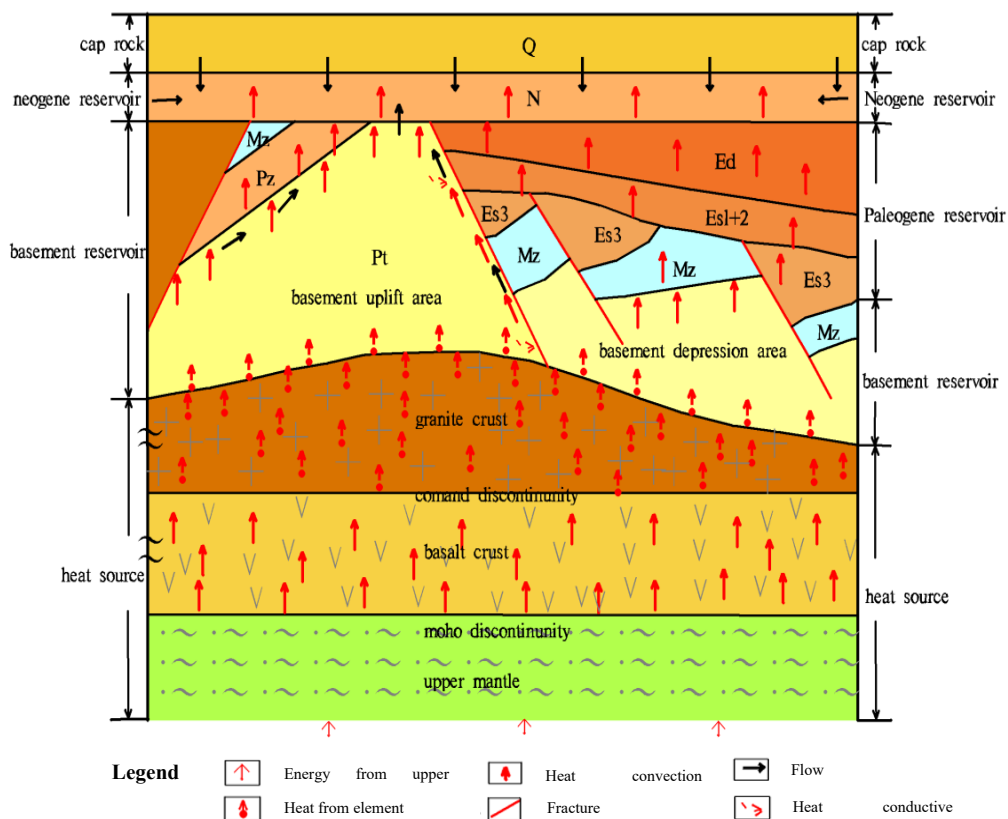


FIGURE 13: The conceptual geological model of Jxw reservoir in Tianjin (Hu Y. et al., 2007; Wang Kun, 2001, Ruan Chuanxia, 2011)

4. Flow path

Permeable faults connect the different formations and act as paths for the geothermal fluids, connecting different depths of the reservoir near the fault zone.

5. Cap rock

The cap rock is unconsolidated Quaternary sediments, which covers Neogene formations. The lithology mainly consists of cohesive soil and sands. The geothermal reservoir is under the cap rock. It has loose structure, large porosity, small density and poor heat conductivity.

4.1.2 Conceptual model of study area

The geothermal reservoir is generally distributed in the western part of Cangdong fault. Drilling has not exposed stratigraphy in the eastern part of Cangdong fault. According to the geophysical data, the buried depth of Jxw reservoir is over 3500 m, so there is no obvious hydraulic connection between the two areas. The western part of the study area was chosen for the conceptual model and numerical model (Figure 14).

There are five layers, from top to bottom: Cenozoic Neogene Nm Group and Ng Group, Cambrian (Hw), Mesoproterozoic Qingbaikou (Q_b) and Jixian Wumishan Group (Jxw). The cap rock is a Quaternary layer with low thermal conductivity and a thickness of 280~320 m. The Nm and Ng layers represent a porous type of reservoir, the horizontal permeability is good, but vertical permeability is low because of interbedded mud layers. The porosity of Hw and Q_b layers is very low in the study area, so these two layers can be combined together as an aquiclude layer, while the porosity of Jxw reservoir is around 5-6%, according to the well data. The exposure depth is from 1850 to 2300 m and the permeability is between 4.9×10^{-13} and $1.25 \times 10^{-13} \text{ m}^2$.

The heat flux emitting from the bottom to the top covers the whole area. Geothermal fluid flows along the Cangdong fault and hot water flows from the deeper parts of the system along the fault and recharges into the shallow parts of the reservoir. The outflow temperature of the Nm wells near the fault is near 80°C, while in the other Nm wells, over 5 km away from the fault, the outflow temperature is only 45-55°C.

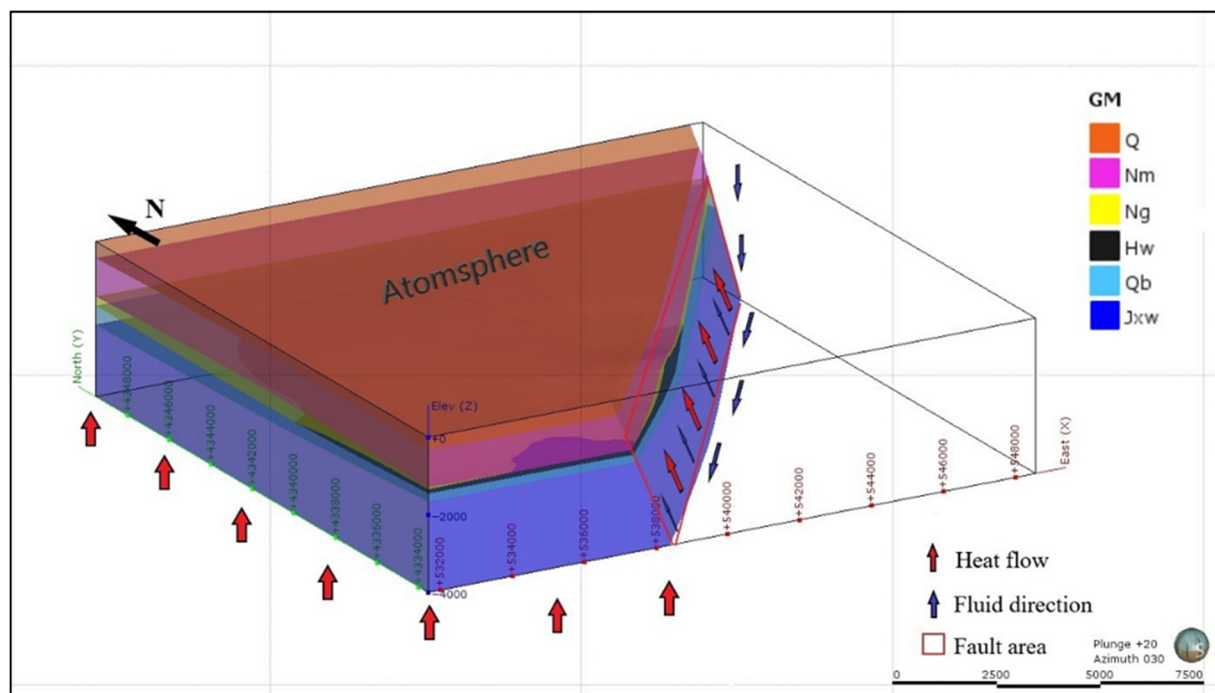


FIGURE 14: The conceptual and numerical model of the study area

4.2 Numerical model

The numerical model was developed like illustrated in Figure 15. The approach allows different components to be adjusted until the model is optimized. The pre-processor software PetraSim was used through the study, as it can establish reservoir models input to TOUGH2 and display calculation results. Due to the time constraints of the project, this study aims at modifying the numerical model to natural state.

4.2.1 Introduction of PetraSim-Tough2

A numerical model was made using PetraSim with TOUGH2 as the core. PetraSim is a set of pre-processing and post-processing programs designed for TOUGH2 that can help users quickly build models and look at simulated results for different purposes (Thunderhead Engineering, 2015). Moreover, PetraSim has integrated TOUGH2MP (parallel computing) into the solution of the equations, improving the speed of the model (Zhang K. et al., 2008). TOUGH2 is a set of procedures for simulating the multidimensional migration of multiphase and multicomponent fluids and heat flow in porous and fractured media. It is mainly used to simulate heat storage, nuclear waste disposal, environmental assessment and remediation, and the flow of fluid or solute migration in variable and saturated media and aquifers (Pruess et al., 1999).

TOUGH2 is used to solve the mass and energy equations describing the migration of fluid and heat flow in multiphase and multicomponent systems. The migration of fluids is described by Darcy's law, and there is a dispersion of matter in all phases. The heat flow is transferred through conduction and convection, and thermal effects are also considered in the convection. The accuracy of TOUGH2 has been compared with laboratory and field analytical solutions and values (Moridis and Pruess, 1992; Pruess et al., 1996).

The mass and energy equations of TOUGH2 can be defined as follows:

$$\frac{d}{dt} \int_{V_n} M^{(\kappa)} dV_n = \int_{\Gamma_n} F^{(\kappa)} \cdot n d\Gamma_n + \int_{V_n} q^\kappa dV_n \quad (1)$$

where V_n is the micro-element in the flow system which is surrounded by the enclosed boundary Γ_n ;
 M is the mass or energy of the unit volumes $\kappa = 1, 2 \dots$;
 NK is the mass component (water, air, H_2 , solute etc.);
 $\kappa = NK + 1$ is thermal component;
 F is mass or heat flow;
 q is the source sink; and
 n is a normal vector of surface elements pointing in the interior of V_n .

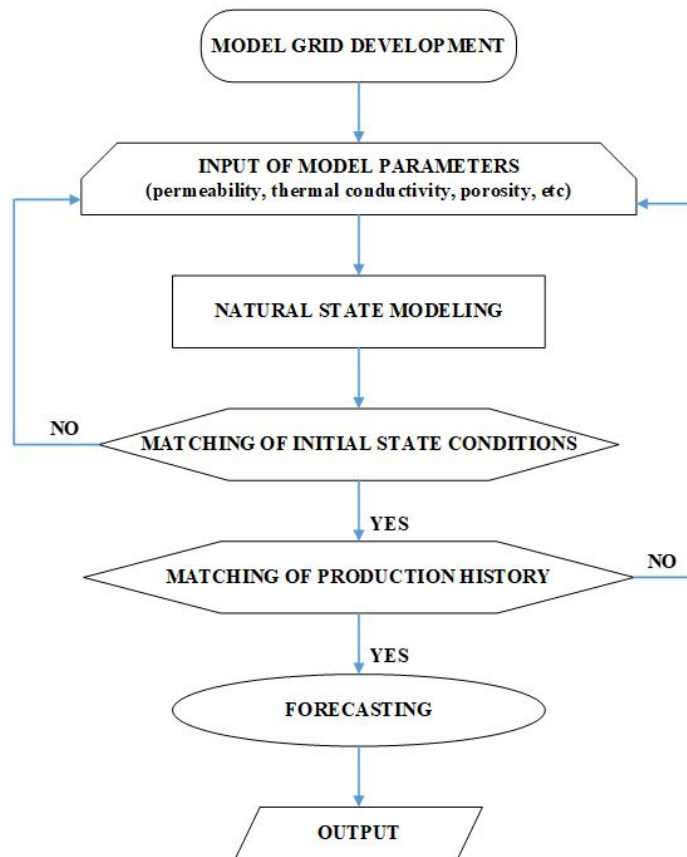


FIGURE 15: Flow chart for development of a numerical model (Ahmed, 2009)

The general form of mass accumulation is:

$$M^K = \phi \sum_{\beta} S_{\beta} \rho_{\beta} X_{\beta}^K \quad (2)$$

where the mass of all the fluid phases can be obtained by summing all the fluid phases β (including liquid, gas and non-aqueous liquid (NAPL));
 Φ is porosity;
 S_{β} is β saturation (the percentage of pore volume);
 ρ_{β} is the density of β ; and
 X_{β}^K is the mass fraction of component K in X-fluid phase β .

The general form of heat accumulation in a number of phases is:

$$M^{NK+1} = (1 - \phi) \rho_R C_R T + \phi \sum_{\beta} S_{\beta} \rho_{\beta} u_{\beta} \quad (3)$$

where ρ_R is the density of rock particles;
 C_R is rock heat capacity;
 T is temperature; and
 u_{β} is internal energy of β .

4.2.2 Layer creation and mesh generation

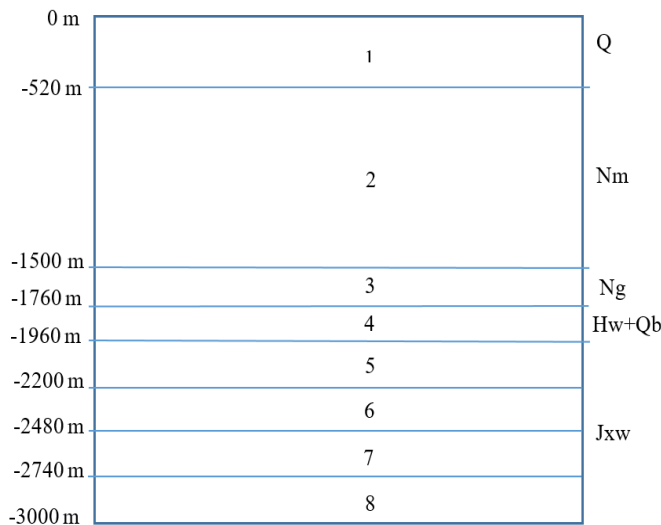


FIGURE 16: Layer distribution of the stratigraphy model in the vertical direction

A stratigraphy model was created as shown in Figure 16, there are eight layers in the vertical direction. The eight layers can be further divided into four parts: the cap rock is layer 1 (0-500 m), the porous reservoir is layers 2 and 3 (500-1760 m), and the aquiclude is layer 4 (1760-1960 m). The Jxw is the main study reservoir, so the layer is split every 260 m into four parts, layers 5-8 (1960-3000 m).

Every layer is horizontally distributed, each layer was assigned a different colour, mesh grids were generated in polygonal shapes and the grid was automatically refined near the well. Maximum cell area is set to $1.7 \times 10^5 \text{ m}^2$, while the grid near the well is 1000 m^2 , the total number of grid units is 17479 (Figure 17).

4.2.3 Boundary conditions

According to the results of isotope analysis, the general flow direction is from the northern mountain area to the southern plain area. Therefore the southern part was set as a constant pressure boundary, the northern and western boundaries were set as constant low-pressure boundaries (Dirichlet boundaries). The cells at the bottom of the model near the Cangdong fault were set as a Neumann boundary. For the natural state there is no source, and the sink boundary is caused by human activities.

The top of the model is a Quaternary layer set as an atmosphere boundary, a very thin layer was created which did not affect the calculation results and the initial value is fixed to $1.013 \times 10^5 \text{ Pa}$ and 13.5°C

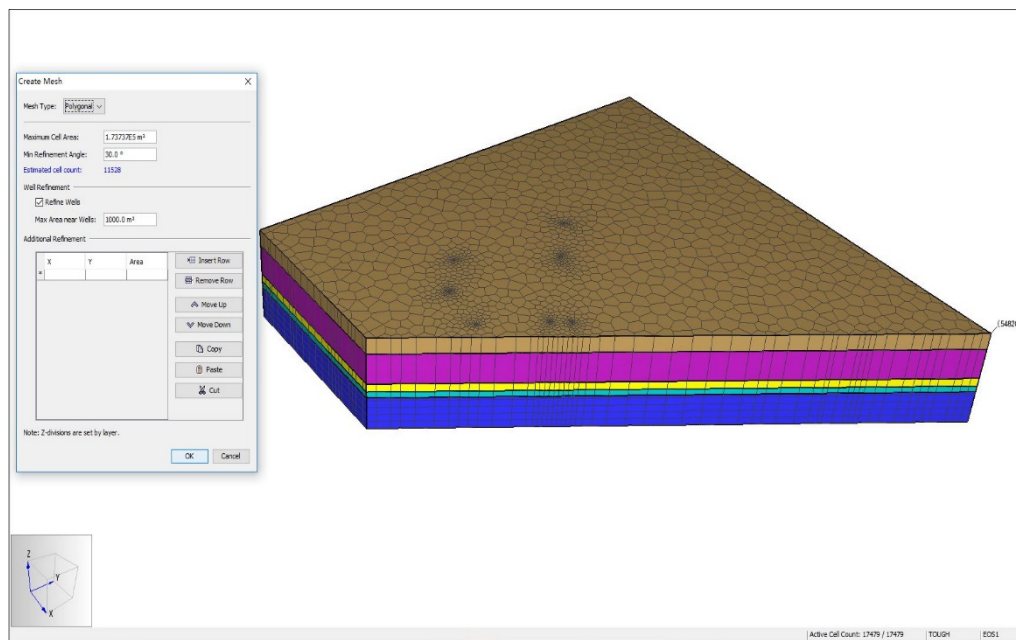


FIGURE 17: Mesh grid generation for the numerical model

(Figure 18). The bottom of the model is set to a constant heat flux boundary. In addition, a very thin layer was created and the value set to $0.2 \text{ J}/(\text{s m}^2)$ (Figure 19) which is the mean value calculated from the different well temperature gradients. The side boundary is set as a heat transfer boundary.

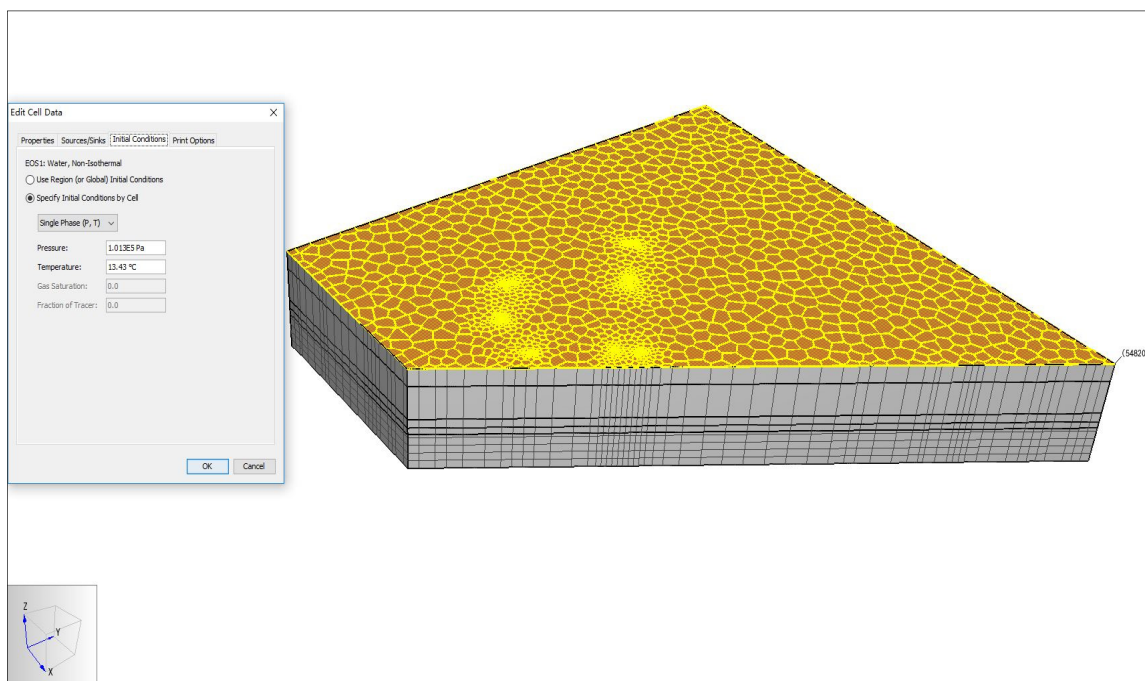


FIGURE 18: Top boundary of the numerical model

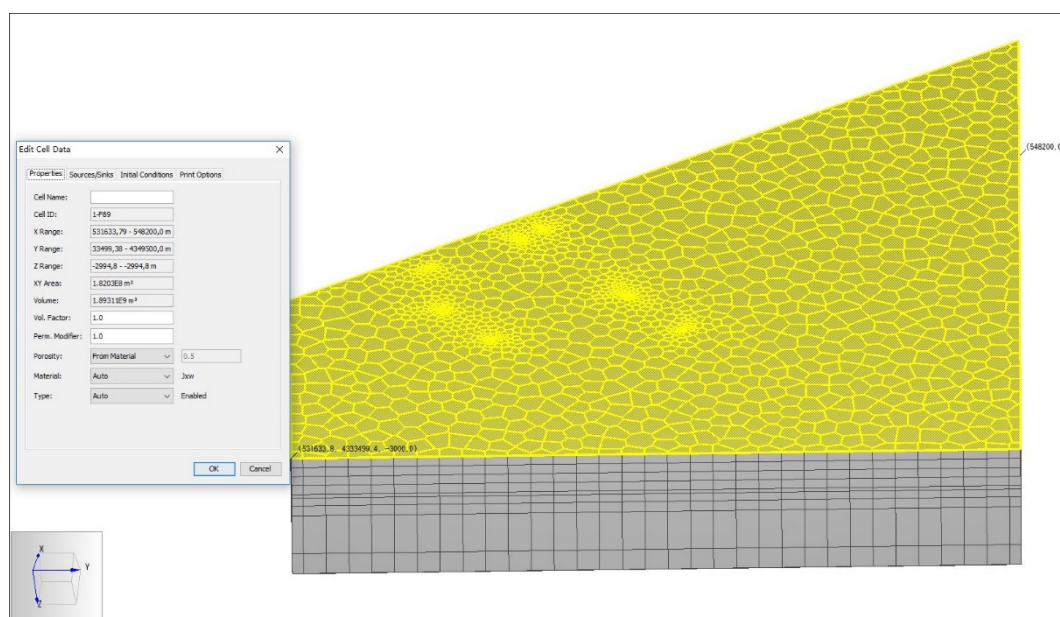


FIGURE 19: Bottom boundary of the numerical model

4.2.4 Parameters selection and initial conditions

PetraSim has many EOS (Equations-Of-State) modules for different phase conditions of the reservoir fluid (Table 4), and each EOS has different variables as presented in Table 4. The outflow temperature of geothermal wells in the study area is generally below 100°C and CO₂ or air content is very low in the fluid, so EOS1 type was selected assuming that there is only fresh water in the reservoir. This is the most basic EOS module, providing a description of fresh water in its liquid and vapour phases. All water properties (density, specific enthalpy, viscosity, saturated vapour pressure) are calculated from the steam table equations as given by the International Formulation Committee (1967) (Thunderhead Engineering, 2015).

TABLE 4: EOS selection through PetraSim

EOS	Description
1	Water, water with tracer
2	Water and CO ₂
3	Water and air
5	Water and hydrogen
7	Water, brine, and air
7R	Water, brine, two radionuclides, and air
9	Saturated-unsaturated flow (used for vadose zone)
EWASG	Water, NaCl, non-condensable gas
ECO2	Water, brine, and CO ₂ for sequestration studies

The parameters, based on measured or assumed values, were put into the numerical model as shown in Table 5. Physical parameters, such as density, specific heat and porosity were fixed because these values were gained from laboratory analysis of rock cores and the numerical model was comparatively insensitive to them. The pressure and temperature distributions were sensitive to permeability and wet heat conductivity, which needed to be calibrated within reasonable range for fitting data (Table 5).

The initial pressure condition was given to each layer as a function according to hydrostatic pressure, and the initial temperature was given by a temperature gradient of 4°C /100 m, as shown in Figure 20.

TABLE 5: Parameter values put into the numerical model

Parameters	Q	Nm	Ng	Qb	Jxw
Density (kg/ m ³)	1980	1930	2012	2760	2677
Porosity (%)	0.2	0.29	0.32	0.1	0.5
Specific heat (J/(kg·K))	1501	1000	1060	1020	1600
X ,Y permeability (m ²)	1.00×10 ⁻¹³	2.00×10 ⁻¹³	2.20×10 ⁻¹³	1.00×10 ⁻¹⁴	3.00×10 ⁻¹³
Z permeability (m ²)	1.00×10 ⁻¹⁵	2.00×10 ⁻¹⁴	2.20×10 ⁻¹⁴	2.00×10 ⁻¹⁶	3.00×10 ⁻¹⁴
Wet heat conductivity (W/(m·K))	0.63	1.1	1.4	2.3	2.6

4.3 Natural state model

Before production, the reservoir has a natural state, a distribution of pressure and temperature without a source and sink caused by exploitation. Using the natural state, the model is run into a quasi-steady state, reproducing the distribution of pressure and temperature, and the distribution is then compared with the measured data. Some parameters are then adjusted, and the model is rerun until a steady state is obtained that is closer to the observed data. The process of adjusting parameters to get a natural state match is usually slow (Ahmed, 2009). There is no fluid recharge to the reservoir except the heat flux from the bottom for the natural state calculation.

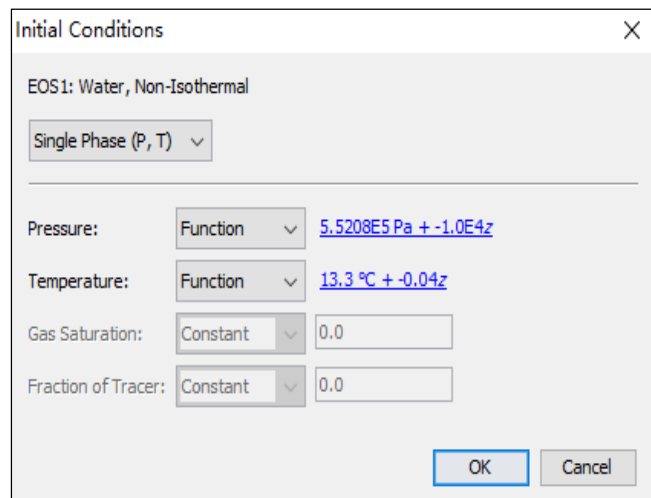


FIGURE 20: Initial condition input into numerical model

The first well drilled in the study area was DL-19 in 1983, so the well logging results of temperature and pressure of this well can be considered as the initial observed data for the model matching the natural state. Taking into account that the evolution of the sedimentary basin geothermal field occurs in a geological history period, the model with EOS1 was executed for 1,000,000 years (1Ma) to reach a quasi-steady state condition (Figure 21).

The comparison graphs between the observed and simulated temperature and pressure data are shown in Figure 22. The results show a big deviation, the simulation temperature is always below the observed data and the mean relative error of the temperature simulation is nearly 20.5%, and for the pressure simulation it is 10.1%.

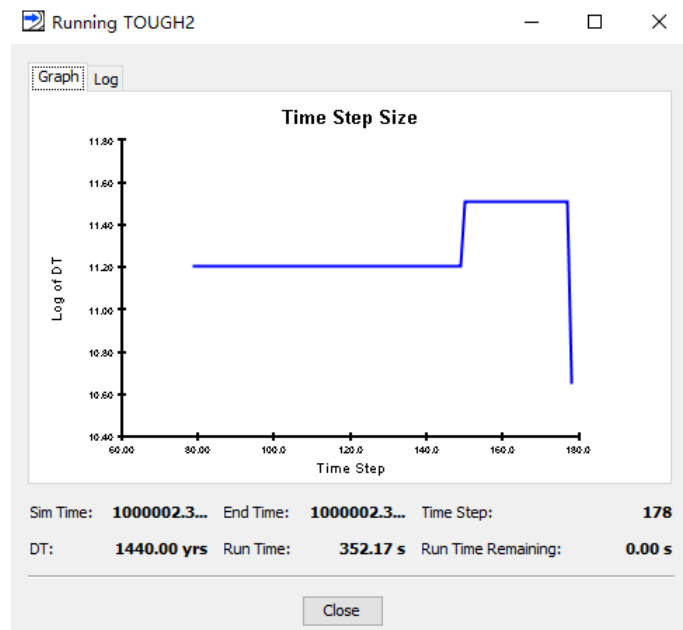


FIGURE 21: Numerical model reaching steady state solution

Permeability and wet heat conductivity were modified for a better fitting with the measured data. After several trials the parameters were chosen according to Table 6.

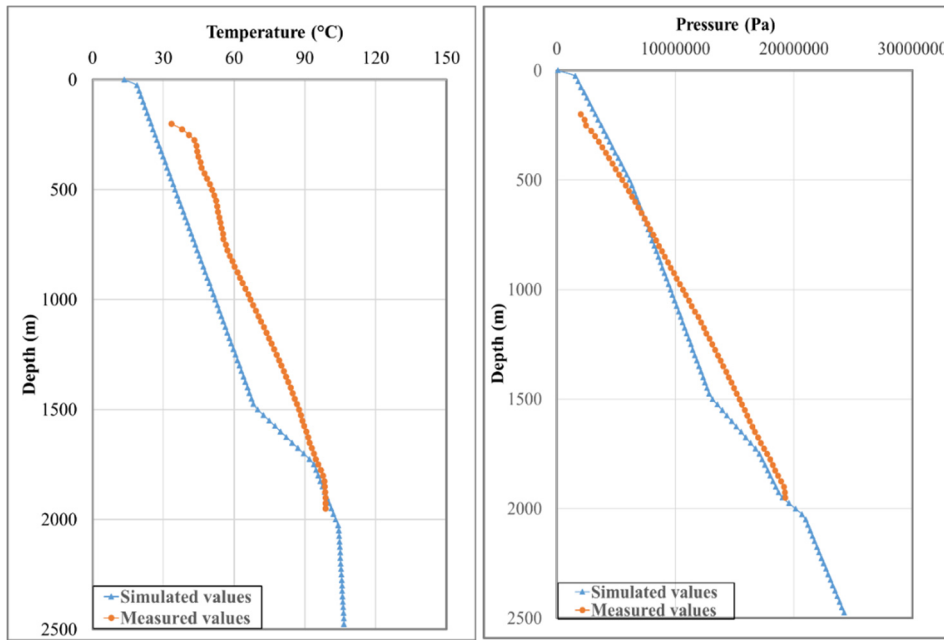


FIGURE 22: Comparison between observed and simulated temperature and pressure for the natural state of the reservoir after the first numerical model

TABLE 6: Calibration parameters for the numerical model

Parameters	Q	Nm	Ng	Qb	Jxw
X ,Y Permeability (m ²)	1.00×10^{-13}	2.00×10^{-12}	2.50×10^{-13}	2.00×10^{-14}	3.00×10^{-13}
Z Permeability (m ²)	1.00×10^{-15}	2.00×10^{-14}	2.50×10^{-15}	2.00×10^{-16}	3.00×10^{-14}
Wet heat conductivity (W/(m·K))	0.63	1.6	1.8	2.5	2.9

After the parameters' calibration, temperature values show less deviation than the pressure values, the mean relative error of the temperature simulation is 3.33% while for the pressure simulation it is 9.73% (Figure 23).

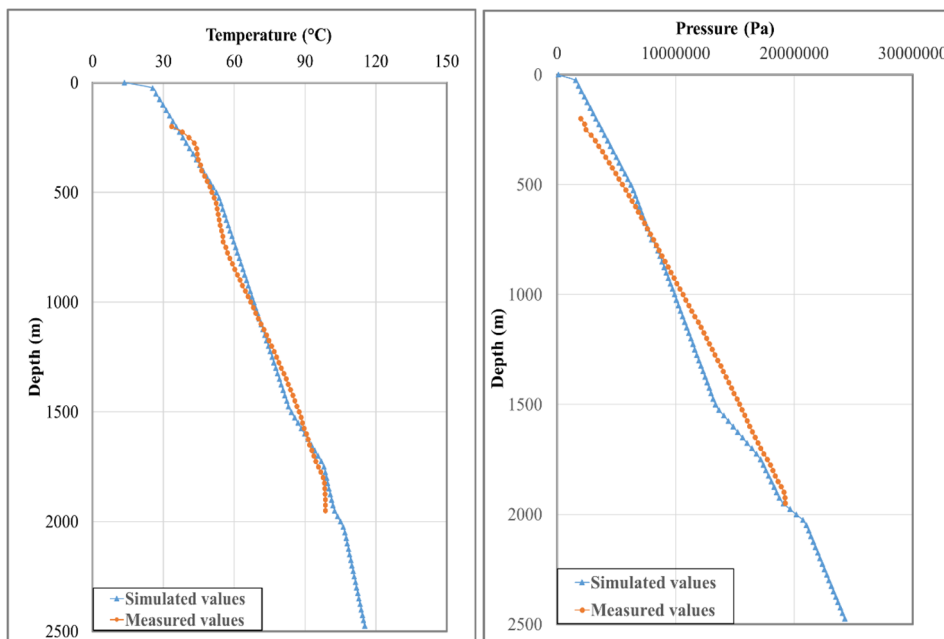


FIGURE 23: Comparison between observed and simulated temperature and pressure for the natural state of the reservoir after calibration of the numerical model

According to the natural state model the distribution of temperature is as shown in Figure 24, the temperature varies from 13.5°C on the surface to 141°C at the bottom.

Pressure distribution in the natural model as shown in Figure 25. The pressure varies from 0.101 MPa on the surface to 28.2 MPa on the bottom, which shows a relatively uniform distribution.

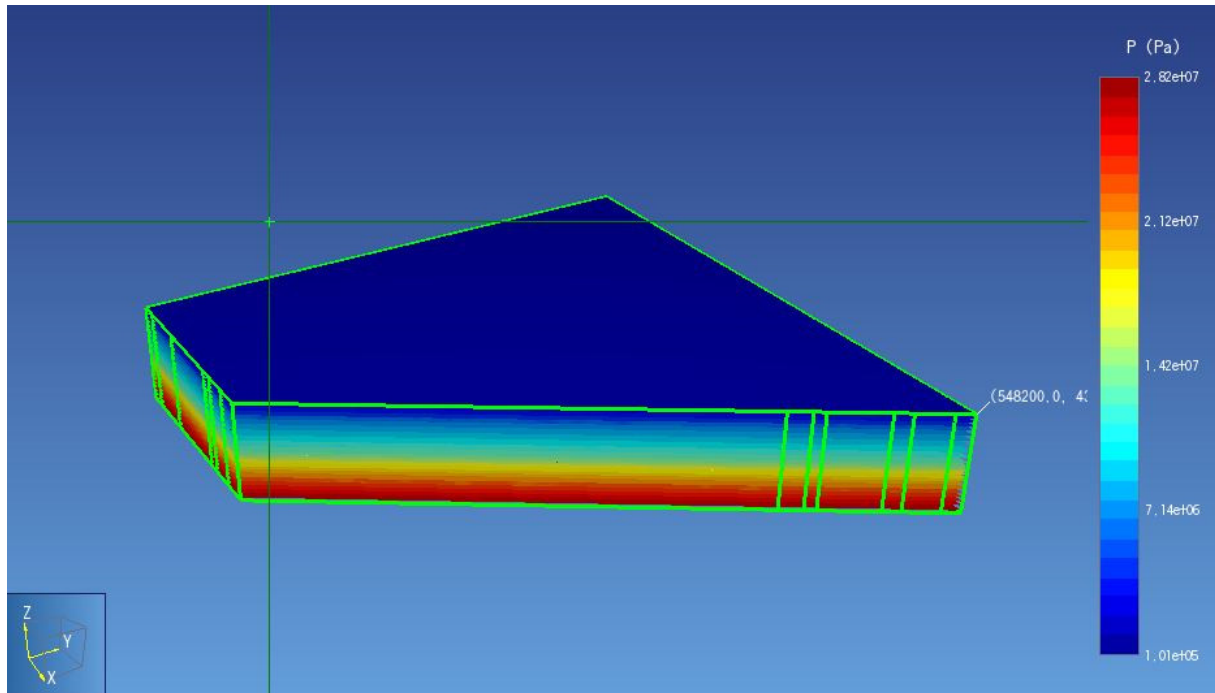


FIGURE 24: Natural state temperature distribution for the calibrated numerical model

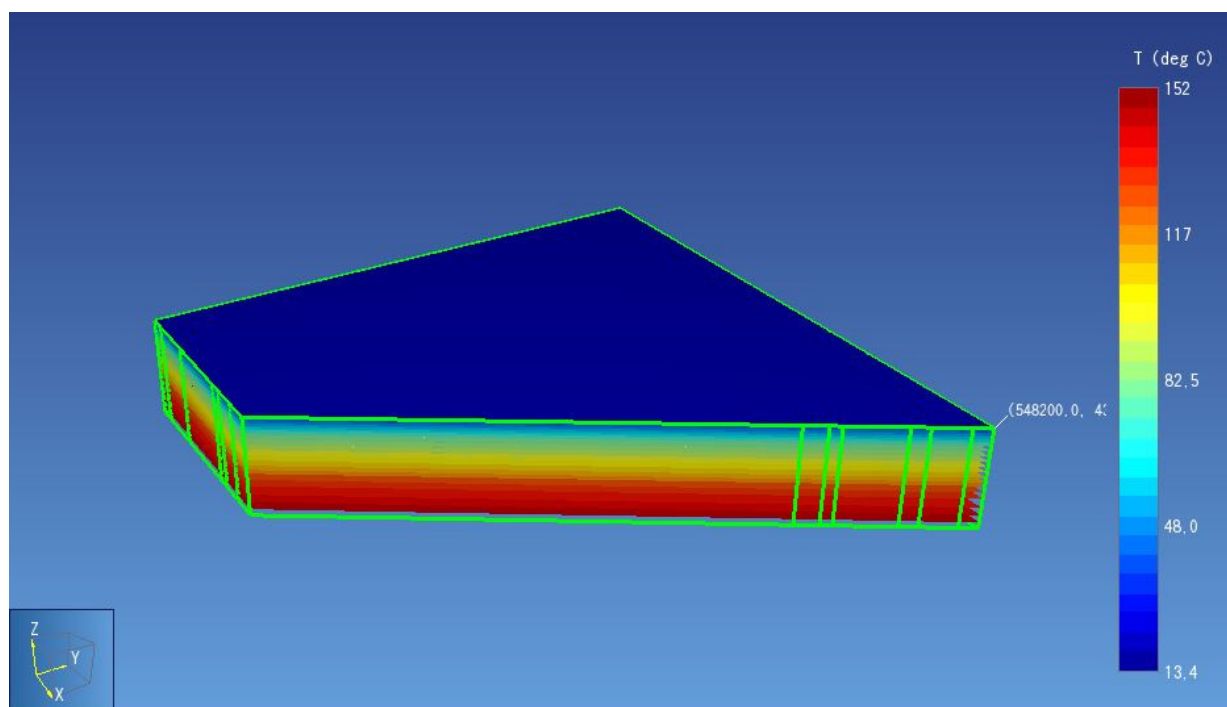


FIGURE 25: Natural state pressure distribution for the calibrated numerical model

5. CONCLUSIONS

A 3D geological model and numerical model were established for the Dongli Lake area in Tianjin Binhai new district, and the main conclusions of the project are as listed below:

- 1) The study area covers 300 km², including the Dongli Lake area. A square shaped 3D geology model was created using Leapfrog Geothermal with different kind of data integrated.
- 2) According to the 3D geology model, from the surface to the bottom the layers revealed are Quaternary, Neogene Nm and Ng formations, Mesozoic, Carboniferous-Permian, Ordovician, Cambrian, Qingbaikou and Jxw formation.
- 3) Two planned wells DL-77 and DL-77B were sited in the western part of the Cangdong fault, where the upper part of the fault area is, and with a low drilling risk. The complete depth of the wells to Jxw reservoir is 2385 m and 2364 m, respectively.
- 4) The heat source comes from the radioactive decay of elements from the deep crust granite and the upper mantle lava flow. The Quaternary layer is the caprock, and Cangdong fault conducts heat and hot fluid from the deeper layers. Jxw is the main reservoir.
- 5) A numerical reservoir model was developed using PetraSim, it covers an area of 182 km². The parameters were input to different layers, and after calibration the observed and simulation data showed a good match, the relative error of the temperature and pressure is 3.33% and 9.73%, respectively, which means the model does represent the natural state. The calibration for the X, Y permeability of the Jxw reservoir is 3.00×10^{-13} m², Z permeability is 3.00×10^{-14} m² and wet heat conductivity is 2.9 W/(m·K).

6. FUTURE WORK

Visualizing all the data in a 3D geology model is very helpful for further interpretation and understanding of the study area. This is expected to be a living model, updated with new data whenever they will be available.

Two planned wells were sited in the study area and a new tracer test should be done there, due to the property of the limestone reservoir. The wells near the study area should also be sampled for tracer test monitoring, followed by a cooling prediction under a different exploitation mode, such as a different time period (rainy season or whole year), different temperature of reinjection water (5-20°C), etc.

According to logging of different geothermal wells and pumping results, parameters partition (permeability, heat flux) should be done to optimize the numerical model. The next step is to put in the natural state as the initial condition to match the model with production history data. Once the model provides satisfactory matching results, different development scenarios can be selected for forecasting, which will provide a basis for the geothermal resource management.

A comparison of cooling predictions between the numerical model and the analytic method should be done. The difference is the reflection of how much the heat flow contributes to the temperature recovery of the reinjection fluid.

ACKNOWLEDGEMENTS

I would like to express my great gratitude to UNU-GTP for offering me the precious opportunity to attend this special training. Thank you so much to the director Mr. Lúdvík S. Georgsson, as well as to all the technical staff of UNU-GTP, Mr. Ingimar G. Haraldsson, Ms. Thórhildur Ísberg and Mr. Markús A.G. Wilde. Special gratitude to Ms. Málfríður Ómarsdóttir for sacrificing her personal time to give us swimming lessons on the weekend.

Sincere thanks to Ms. Vaiva Čypaitė, Ms. Valdís Guðmundsdóttir, Dr. Guðni Axelsson and Ms. Saeunn Halldórsdóttir from ÍSOR, for their supervision and guidance during the preparation of the personal project. Thanks for giving me patient guidance and advice, and sharing knowledge and experience – thanks for all the help and assistance.

Thanks Mr. Cheng Wanqing, Mr. Lin Li and Mr. Zhao Sumin for recommending me for participation in this training. I am greatly indebted to all my staff members in Tianjin Geothermal Exploration and Development Designing Institute.

Special thanks go to Dr. Li Yiman and Ms. Zheng Tingting for giving me a family feeling in Iceland. See you in China.

Finally, I express my deepest love to my wife and my daughter. It is because of their strong support that I could finish my studies in Iceland.

REFERENCES

Ahmed, H., 2009: *Numerical simulation of Germencik geothermal field*. Middle East Technical University, Turkey, MSc thesis, 79 pp.

Axelsson, G., 2008: Management of geothermal resources. *Proceedings of the Workshop for Decision Makers on the Direct Heating Use of Geothermal Resources in Asia, organized by UNU-GTP, TBLRREM and TBGMED*, Tianjin, China, 15 pp.

Axelsson, G., 2010: Sustainable geothermal utilization – case histories, definitions, research issues and modelling. *Geothermics*, 39, 283–291.

Axelsson, G., 2012: Role and management of geothermal reinjection. *Proceedings of the “Short course on geothermal development and geothermal wells”, organized by UNU-GTP and LaGeo, Santa Tecla, El Salvador*, UNU-GTP SC-14, 21 pp.

Axelsson, G., 2013: Geothermal well testing. *Proceedings of the “Short Course on Conceptual Modelling of Geothermal Systems”, organized by UNU-GTP and LaGeo, Santa Tecla, El Salvador*, ?? pp.

Duan Z., Pang Z., and Wang X., 2011: Sustainability evaluation of limestone geothermal reservoirs with extended production histories in Beijing and Tianjin, China. *Geothermics*, 40, 125–135.

Grant, M.A., Donaldson, I.G., and Bixley, P.F., 1982: *Geothermal reservoir engineering*. Academic Press, NY, 369 pp.

Gunnarsdóttir, S.H., and Poux, B., 2016: *3D modelling of Hellisheidi geothermal field using Leapfrog: data, workflow and preliminary models*. Orkustofnun, Reykjavik, report OS-88041/JHD-06, 22 pp.

Hu Y., Lin L., Lin J., Cheng W., Zhao S., and Yu Y., 2007: *Report about the potential evaluation of the sustainable development of geothermal resources in Tianjin*. Tianjin Geothermal Exploration and Development Designing Institute, report (in Chinese), 213 pp.

Thunder Head Engineering, 2015: *PetraSim User Manual*. Thunder Head Engineering, Manhattan, NY, US.

Leapfrog, 2017: *3D geological modelling software*. Leapfrog, webpage: www.leapfrog3d.com/

Moridis, G., and Pruess K., 1992: *TOUGH simulations of Updegraff's set of fluid and heat flow problems*. Lawrence Berkeley Laboratory, report LBL-32611, Berkeley, CA.

Pruess K., Oldenburg C., Moridis G., 1999: *Tough2 user's guide, version 2.0*. Earth Sciences Division, Lawrence Berkeley National Laboratory, University of California, Berkeley, CA, USA, 198 pp.

Pruess K., Simmons A., Wu Y. S., and Moridis, G., 1996: *TOUGH2 Software Qualification*. Lawrence Berkeley National Laboratory report LBL-38383, Berkeley, CA.

Ruan Chuanxia, 2011: Numerical modelling of water level changes in Tianjin low-temperature geothermal system, China. Report 31 in: *Geothermal training in Iceland 2011*. UNU-GTP, Iceland, 775-798.

Tian G., 2014: *Sustainable development and utilization of geothermal resources in the Dongli Lake resort in Tianjin* (in Chinese). China University of Geosciences, Beijing, MSc thesis, 106 pp.

Tianjin Bureau of Geology, 1992: *Tianjin regional geological records*. Geology Press, Beijing, 190 pp.

Wang Kun, 2001: Application of isotopic techniques on establishing hydrothermal concept model. *J. Science in China*, Dec., 4.

Wang Wanli, 2016: Modelling of tracer tests in a geothermal reservoir in Tianjin, China. Report 41 in: *Geothermal training in Iceland 2016*. UNU-GTP, Iceland, 891-910.

Zhang K., Wu Y., and Pruess K., 2008: *User's guide for TOUGH2-MP—A massively parallel version of the TOUGH2 Code*. Earth Sciences Division, Lawrence Berkeley National Laboratory, University of California, Berkeley, CA, USA, 108 pp.

Zhao Na, 2010: Geothermal simulation of lake water injection into the geothermal reservoir in Tianjin, China. Report 32 in: *Geothermal training in Iceland 2010*. UNU-GTP, Iceland, 711-730.

Zong Z., Yan J., Wang B., Zhang S and Yin X., 2016: *The annual report of dynamic monitoring of geothermal resources in Tianjin*. Tianjin Geothermal Exploration and Development Designing Institute, report (in Chinese), 152 pp.